EXHIBIT 2

Oncolytic Herpes Simplex Virus Vector Therapy of Breast Cancer in C3(1)/SV40 T-antigen Transgenic Mice

Renbin Liu, Susan Varghese, and Samuel D. Rabkin

Molecular Neurosurgery Laboratory, Massachusetts General Hospital and Harvard Medical School, Charlestown, Massachusetts

Abstract

Oncolytic herpes simplex virus vectors are a promising strategy for cancer therapy, as direct cytotoxic agents, inducers of antitumor immune responses, and as expressers of anticancer genes. Progress is dependent upon representative preclinical models to evaluate therapy. In this study, two families of oncolytic herpes simplex virus vectors (G207 and NV1020 series) that have been in clinical trials were examined for the treatment of breast cancer, using the C3(1)/T-Ag transgenic mouse model. Female mice spontaneously develop mammary carcinomas, and the C3(1)/T-Ag–derived tumor cell line M6c forms implantable tumors. Both *in vitro* and *in vivo*, G47Δ, derived from G207 by deletion of ICP47 and the US11 promoter, was more efficacious than G207. Whereas NV1023, derived from NV1020 by deletion of ICP47 and insertion of LacZ, was as cytotoxic to M6c cells *in vitro* as G47Δ, it did not inhibit the growth of s.c. M6c tumors but did extend the survival of intracerebral tumor bearing mice. In contrast, NV1042, NV1023 expressing interleukin 12, inhibited s.c. M6c tumor growth to a similar extent as G47Δ, but was less effective than NV1023 in intracerebral tumors. In the spontaneously arising mammary tumor model, when only the first arising tumor per mouse was treated, G47Δ inhibited the growth of a subset of tumors, and when all tumors were treated, G47Δ significantly delayed tumor progression. When the first mammary tumor was treated and the remaining mammary glands removed, NV1042 was more efficacious than G47Δ at inhibiting the growth and progression of injected tumors. (Cancer Res 2005; 65(4): 1532-40)

Introduction

Breast cancer incidence has continued to increase in the United States, albeit at diminished rates (1). Encouragingly, the mortality rate has been decreasing since 1990 (2). Both these trends are thought to partially reflect increased mammography use. Unfortunately, the latest 5-year survival rate for metastatic disease is only 20.4%, compared with 97.5% for localized disease (2). In about 15% to 30% of patients, the primary cancer will metastasize to the brain (3), with this percentage increasing over the last few decades, related in part to longer survival due to increased efficacy of current treatments of peripheral disease (4). Surgery is the primary treatment for localized tumors, often with radiation, followed by adjuvant chemotherapy and hormonal therapy, depending upon receptor status (5), and more recently biological therapies that target the epidermal growth factor receptor family and downstream signaling (6). Metastasis to the brain frequently results in severe and debilitating neurologic complications, which have a large impact on a patient's quality of life. Therapy for metastatic disease is often only palliative (5) and has minimal effect on survival in patients with brain metastases (7).

Oncolytic viruses are promising therapeutic agents for cancer. They are inherently cytotoxic to tumor cells and conditionally replicative so that spread of the vector is confined to the tumor (8). Major advantages of such vectors are *in situ* amplification and spread within the tumor, ability to transfer therapeutic transgenes to the tumor, and induction of antitumor immune responses. Of course, equally important for clinical translation is that such vectors have minimal toxicity to normal tissue. Herpes simplex virus (HSV) has many properties that make it an attractive cancer therapeutic agent and it has served as a prototypic oncolytic virus (9). A variety of oncolytic HSV vectors have been developed, with three among these, G207, 1716, and NV1020, safely completing phase 1 clinical trials (9).

In this paper, we examine the efficacy of oncolytic HSV vectors from the G207 and NV1020 series. G207 is a multigene mutant of HSV-1 that contains deletions of both copies of the γ34.5 gene, the major viral determinant of neurovirulence (10) and antagonist of activated double-stranded RNA-dependent protein kinase R (11), and an *Escherichia coli LacZ* insertion that inactivates the *ICP6* gene (*UL39*), encoding the large subunit of ribonucleotide reductase, a key enzyme in nucleotide metabolism and viral DNA synthesis in nondividing cells (12, 13). G207 is efficacious in the treatment of multiple human tumors in athymic mice and mouse tumors in syngeneic animals, yet is nonpathogenic to HSV-sensitive mice and nonhuman primates (14). In addition to its oncolytic activities, G207 infection of tumor cells in immunocompetent mice induces a systemic and specific antitumor immune response (15–18). Whereas the mutations in G207 confer significant safety attributes (13), they also attenuate viral growth.

To enhance the antitumor activities of G207, we generated G47Δ, which contains an additional deletion of the nonessential α47 gene (ICP47; ref. 19). Because of the overlapping transcripts encoding ICP47 and US11, this deletion places the late US11 gene under control of the immediate-early α47 promoter, which results in an enhancement of growth of γ34.5 mutants and broadens the range of susceptible tumor cells by precluding the shutoff of host protein synthesis (20). ICP47 binds to the transporter associated with antigen presentation (TAP) and blocks peptide loading of MHC class I molecules (21). Its deletion, therefore, leads to increased MHC class I presentation on infected cells, enhanced stimulation of lymphocytes, and decreased NK cytolysis (19, 22), which should augment the induction of an immune response. Unfortunately, ICP47 is unable

to inhibit rodent TAP, making mice an unsuitable model to examine the impact of ICP47 *in vivo* (23).

NV1020 (previously called R7020) is a HSV-1/HSV-2 intertypic recombinant that was developed and unsuccessfully tested in humans as a herpes vaccine (24, 25). It contains a large deletion of the joint region, including *UL56* and one copy of $\gamma 34.5$, a duplication of *UL5* and *UL6*, insertion of HSV-2 *gJ*, *gG*, and *PK*, and deletion of *UL24* (24, 26). Because it is not attenuated for neuroinvasiveness, it has been tested against non-CNS tumors (27), including colon cancer metastatic to the liver in mice and humans (28, 29). NV1023 is derived from NV1020 by repairing the *thymidine kinase/UL24* region, and insertion of *E. coli LacZ* into the *ICP47* region, deleting *ICP47* and *US11* (30). This vector was used as the backbone to generate NV1042, which expresses murine interleukin (IL)-12 (30). IL-12 expression has previously been shown to enhance the efficacy of oncolytic HSV therapy and augment the antitumor immune response generated (30–32).

Representative animal models are central to the development and testing of novel therapeutic strategies. As a model for breast cancer, we have used the C3(1)/T-Ag transgenic mouse, which spontaneously develops mammary adenocarcinoma in female mice due to the expression of SV40 large T- and small t-Ag driven by the rat prostatic steroid binding protein C3(1) enhancer/promoter (33, 34). Transgene expression is not estrogen responsive, although estrogen promotes tumorigenesis, so tumor development is not pregnancy or hormone dependent (35). These transgenic mice typically develop atypical hyperplasia in the ducts at about 2 months of age, followed by high-grade mammary intraepithelial neoplasia at 3 months and adenocarcinomas beginning at 4 months (34). Breast cancer cell lines have been established from these mice that form tumors after implantation into heterozygous C3(1)/T-Ag mice (36), including intracerebral tumors that are a model for metastatic disease to the brain. Here, we compared the efficacy of G47Δ and NV1023 in implanted s.c. and intracerebral breast cancer tumors, and determined the impact of IL-12 expression on oncolytic HSV therapy of both implanted (s.c. and intracerebral) and spontaneous mammary tumors. To our knowledge this is the first described treatment of spontaneously arising tumors by oncolytic viruses.

Materials and Methods

Cells and Viruses. M6, M6c, and Pr14-2 tumor cells (obtained from Dr. J. Green, National Cancer Institute, Bethesda, MD) isolated from C3(1)/T-Ag tumors (36, 37) and Vero (African green monkey kidney; obtained from D. Knipe, Harvard Medical School, Boston, MA) cells were cultured in DMEM with glucose (4.5 g/L; Mediatech, Inc., Herndon, VA) supplemented with 10% calf serum (Hyclone Laboratories, Logan, UT) at 37.5°C in 5% CO_2.

G207 and G47Δ were constructed as described (13, 19). NV1023, derived from NV1020 (R7020), contains an insertion of *LacZ* into the *ICP47* locus, deleting *ICP47*, *US11*, and *US10* (30). NV1042 is NV1023 with an insertion of murine IL-12 cDNA (p35 and p40 as a single polypeptide separated by elastin motifs) expressed from a hybrid $\alpha 4$-*TK* promoter (30). Purified virus stocks in Dulbecco's PBS/10% glycerin were provided by MediGene, Inc. (San Diego, CA). Viruses were titered by plaque assay on Vero.

In vitro **Cytotoxicity.** Cells were seeded in 6-well plates at 1×10^5 cells per well. After a 24-hour incubation at 37.5°C, cells were infected with virus at a multiplicity of infection (MOI) of 0.1, whereas controls were Mock infected. The infected cells were incubated at 37.5°C until counting, when they were washed twice with PBS, trypsinized and counted with a Coulter counter (Beckman Coulter, Fullerton, CA).

Animal Studies. Six-week-old female C3(1)/T-Ag heterozygous transgenic mice were purchased from the National Cancer Institute (Frederick, MD) and caged in groups of five or less. Mice were genotyped using the online Jackson Laboratory genotype protocol with primers for T-Ag (5'-CAGAGCAGAATTGTGGAGTGG-3' and 5'-ACAAAC-CACAACTAGAATGCAGTG-3'). Because M6c cells still express T-antigen, they only form tumors in C3(1)/T-Ag transgenic mice. For injections and surgical procedures, each mouse was anesthetized with an i.p. injection of 0.20 to 0.25 mL solution consisting of 86% saline, 9% sodium pentobarbital, and 5% ethyl alcohol. Animal procedures were approved by the Massachusetts General Hospital Animal Care and Use Committee. All animal studies were blinded.

S.c. Tumor Model. M6c cells (1×10^6 in 50 μL of serum-free DMEM) were injected s.c. into the right flank of 6-week-old female heterozygous C3(1)/T-Ag transgenic mice. When s.c. tumors reached approximately 6 mm in maximal diameter, 20 μL of virus (2×10^7 plaque-forming units, pfu) or vehicle (Mock) was inoculated into the tumor (day 0), followed by repeat injections either on days 6 and 11 (G207) or on days 3, 7, and 10 (G47Δ, NV1023, and NV1042). Tumor size was measured by external caliper twice a week and the tumor volume calculated (length × width × height). If animals seemed moribund or the diameter of their tumors exceeded 21 mm, they were sacrificed and this was recorded as the date of death for survival studies.

Intracerebral Tumor Model. Intracerebral tumors were generated by injecting 2×10^3 M6c cells in 4 μL of serum-free DMEM stereotactically into the right frontal lobe of female heterozygous C3(1)/T-Ag mice (38). After 10 days, 4 μL of virus (2×10^6 pfu) or vehicle (Mock) was inoculated stereotactically at the same coordinates, and survival was monitored. Survival was statistically evaluated by Kaplan-Meier analysis and log-rank test (StatView).

Spontaneously Arising Mammary Tumors. Female heterozygous C3(1)/T-Ag transgenic mice spontaneously develop mammary tumors that are palpable from about 4 months of age. Mice with palpable mammary tumors were randomly divided into two groups based on the order of tumor development. We used three treatment paradigms: (a) Only the first mammary tumor to arise was injected with G47Δ (1×10^7 pfu/20 μL) or Mock (10% glycerol in PBS) weekly until the animals were sacrificed due to overall tumor burden; (b) All tumors as they arose were injected with G47Δ (1×10^7 pfu/20 μL) or Mock (10% glycerol in PBS) weekly until the animals were sacrificed due to overall tumor burden; and (c) The first mammary tumor to arise was injected with G47Δ or NV1042 (2×10^7 pfu/20 μL) or Mock (10% glycerol in PBS) weekly. Following the first treatment (about 3 days later), the remaining nine mammary glands were surgically removed. Animals were followed until sacrifice due to overall tumor burden. Tumor sizes were measured with calipers twice a week and the volume (length × width × height) determined. In all cases, both the treatments and measurements were blinded. Statistical differences in tumor growth were assessed using an unpaired *t* test and time to progression using a log-rank test of Kaplan-Meier estimates (Prism, GraphPad Software, Inc., San Diego, CA). The time to progression is based on the Response Evaluation Criteria in Solid Tumors criteria, where a 30% increase in maximal diameter in a spherical tumor will result in a new volume $4/3\pi \times (1.3r)^3$ or $2.2 \times$ the original volume, a 120% increase in volume (39). For the rapidly growing spontaneous tumors, the 30% increase in maximal diameter is more appropriate than the standard 20% increase (or 73% increase in volume) used in clinical trials as the determinant of progressive disease for tumor response evaluation (39).

Histology. Mice were sacrificed and perfused with Zamboni's fixative [1.8% paraformaldehyde, 7.5% picric acid, 0.19% EGTA and 2 mmol/L magnesium chloride (pH 7.3)]. Tumor samples were harvested, frozen with dry ice, and cryostat sections of 20-μm thickness were prepared. Sections were fixed in 2% paraformaldehyde/PBS for 10 minutes, washed twice in PBS, incubated with PBS containing 2 mmol/L magnesium chloride, 0.01% sodium deoxycholate, and 0.02% NP40 at 4°C for 10 minutes, and then stained with substrate solution [PBS (pH 7.2) containing 1 mg/mL 5-bromo-4-chloro-3-indolyl-β-D-galactopyranoside

(X-gal), 5 mmol/L potassium ferricyanide, 5 mmol/L potassium ferrocyanide, 2 mmol/L magnesium chloride, 0.01% sodium deoxycholate, and 0.02% NP40] at 34°C for 4 hours. Sections were washed with PBS/2 mmol/L EDTA and counterstained with H&E before mounting.

Results

In vitro **Cytotoxicity.** To assess the susceptibility of murine breast cancer cells to oncolytic HSV vector cytotoxicity and replication before *in vivo* experimentation, monolayers of C3(1)/T-Ag tumor cells were infected with G207, G47Δ, NV1023, and NV1042 at low MOI (Fig. 1A). M6 cells were established from a spontaneously arising mammary adenocarcinoma in C3(1)/T-Ag mice (36), M6c cells from a lung metastasis arising after s.c. implantation of M6 cells (36), and Pr14-2 from a prostate adenocarcinoma arising in a male C3(1)/T-Ag mouse (37). G47Δ was more effective than G207 at killing all three tumor cell lines, with >60% of cells killed within 3 days at a low MOI of 0.05 (Fig. 1A). At high MOI (=1), both G207 and G47Δ killed M6 and M6c cells within 2 days (data not shown). NV1023 was similarly cytotoxic as G47Δ toM6c cells but was not effective in the parental M6 cells (Fig. 1A).

Treatment of S.c. Tumors. M6c cells were used for the *in vivo* studies because they were more susceptible to oncolytic HSV vector replication *in vitro* than M6 cells, and M6 had highly variable tumor growth rates after s.c. implantation. S.c. M6c tumors were established in female C3(1)/T-Ag heterozygous mice and then injected intratumorally with vector. Similar to what was seen *in vitro*, G207 was unable to inhibit the growth of s.c. M6c tumors (Fig. 1B, *left*) or to extend survival (data not shown). We next examined the efficacy of G47Δ, which significantly inhibited the growth of s.c. M6c tumors (*P* < 0.05, Student's *t* test; Fig. 1B, *middle*). In contrast, NV1023, which replicated well in M6c cells *in vitro*, had no significant effect on M6c s.c. tumor growth (Fig. 1B, *right*). Previous studies from our laboratory have

shown that intratumoral expression of IL-12 significantly enhances antitumor efficacy of oncolytic HSV vectors (31). Similarly here, NV1042 was more efficacious than NV1023 and significantly inhibited s.c. tumor growth (*P* < 0.05, Student's *t* test; Fig. 1B, *right*). Both G47Δ and NV1042 significantly extended the survival of treated mice bearing s.c. tumors, with a mean survival of 44 and 43 days respectively, compared with Mock with a mean of 38 days [*P* < 0.05, log-rank (Mantel-Cox) test], whereas NV1023 had no significant effect.

Intracerebral Tumors. As a model for metastatic breast cancer in the brain, we established M6c intracerebral tumors in female C3(1)/T-Ag heterozygous mice. Cells were implanted stereotactically into the striatum (Fig. 2A) and within 10 days multifocal tumors developed (Fig. 2D). To determine whether G47Δ replication was occurring *in vivo*, intracerebral M6c tumors were treated 10 days post-implantation, animals sacrificed 1, 2, and 4 days after virus injection, and X-gal histochemistry done on sectioned brains to detect infected cells that contain replicating G47Δ. Large numbers of X-gal-positive tumor cells were seen within 24 hours of G47Δ injection (Fig. 2B) and at 2 days (Fig. 2C) and 4 days (Fig. 2D and E) post-infection, with virus staining predominantly surrounding areas of tumor necrosis.

We next examined the treatment of established intracerebral M6c tumors with G47Δ in both young mice (~7 weeks of age), a standard model, and in older mice (~9 months of age), more representative of the clinical situation. G47Δ or vehicle (Mock) was stereotactically injected at the same coordinates as the tumor cells and mice followed until moribund, when they were sacrificed. G47Δ significantly extended the survival of tumor-bearing animals at both ages (*P* < 0.005; log-rank [Mantel-Cox] test; Fig. 2F and G). When we compared the efficacy of NV1023 with NV1042 in the intracerebral tumor model, NV1023 was more effective (Fig. 2H), as opposed to the observation in the
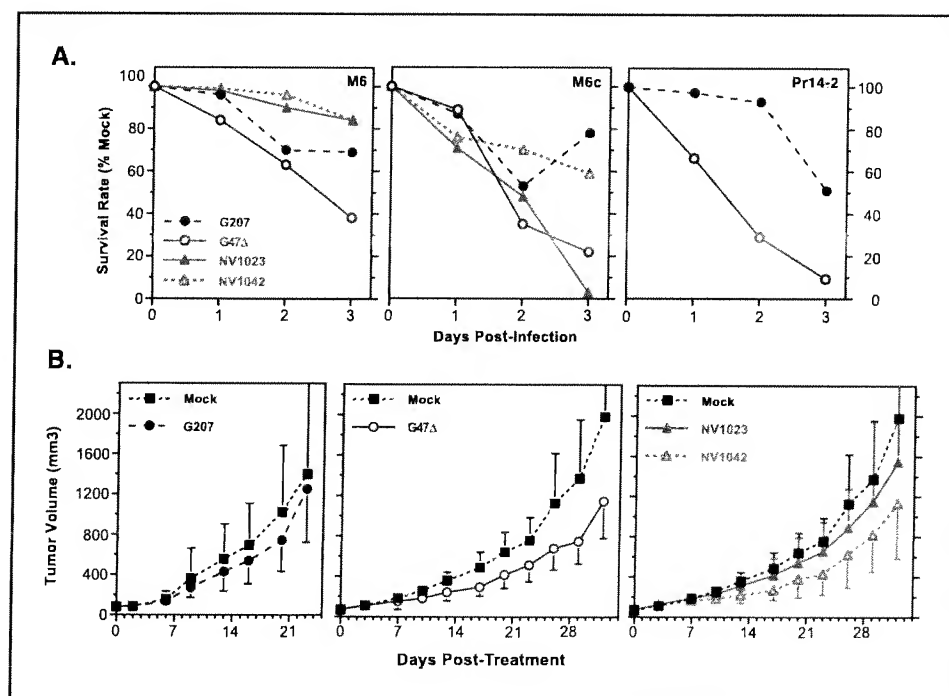
Figure 1. Oncolytic HSV treatment of C3(1)/T-Ag tumor cells. *A, in vitro* susceptibility of murine C3(1)/T-Ag tumor cells to oncolytic HSV vectors. Monolayers of M6 (*left*) and M6c (*middle*) cells were infected with G207, G47Δ, NV1023, or NV1042 at a MOI = 0.05, and Pr14-2 cells (*right*) with G207, G47Δ at a MOI = 0.1, or Mock, and incubated in DMEM/1% heat-inactivated FCS at 37.5°C for the time indicated. Average from duplicate or triplicate (Pr14-2) wells. *B,* treatment of s.c. M6c tumors. M6c cells were implanted s.c. in the right flank of female C3(1)/T-Ag heterozygous mice. *Left,* when tumors were palpable (7 days after implantation), they were injected intratumorally with G207 (2 × 10⁷ pfu/20 μL) or Mock (PBS/10% glycerol) on days 0, 6, and 11 (post-treatment). In a second experiment (*middle* and *right*), palpable tumors (13 days after implantation) were injected intratumorally with G47Δ, NV1023, NV1042 (2 × 10⁷ pfu/20 μL) or Mock (PBS/10% glycerol) on days 0, 3, 7, and 10 (post-treatment). *Points, n = 7 (left)* or *n = 9 (middle and right)* animals per group; *bars,* SD. Tumors treated with G47Δ and NV1042 were significantly smaller than Mock from 10 days post-treatment (*P* < 0.05, Student's *t* test). There was no significant difference between G207 or NV1023 and Mock.
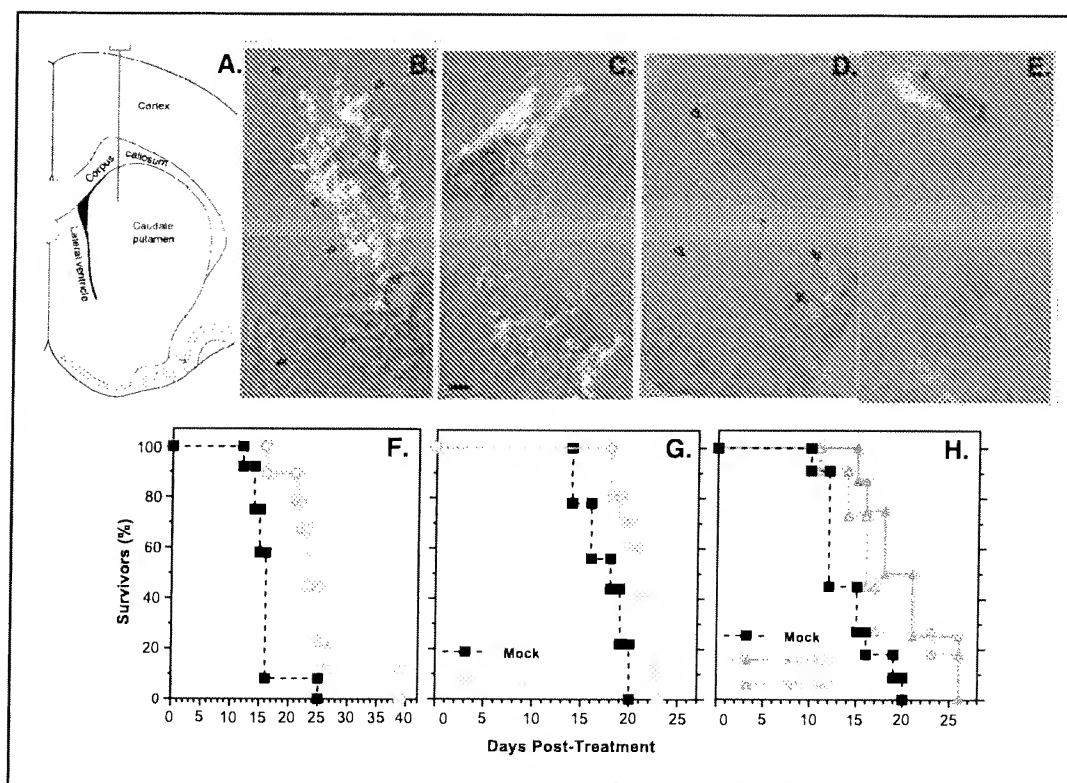
Figure 2. Treatment of breast cancer metastatic to the brain. (*top*) Stereotactic injection of G47Δ into intracerebral M6c tumors. *A*, cartoon of coronal section through mouse brain illustrating the position of tumor cell and HSV injection. *B*, coronal section through brain of mouse 24 hours after G47Δ (2 × 10⁶ pfu) injection and 14 days after M6c cell implantation. Sections were stained with X-gal to identify cells containing replicating G47Δ (*△, blue*), and counterstained with hematoxylin and eosin (tumor deposits, *arrow*). *C*, 48 hours after G47Δ injection. *D*, 4 days after G47Δ injection. *E*, higher magnification of area indicated in *D*. In all cases, the orientation is as in *A*. X-gal-positive cells (*blue*) surrounding tumor deposits can be seen in *B*, *C*, *D*, and *E*. Bar, 0.2 mm in *B*, *C*, and *E*. *Bottom*, oncolytic HSV treatment of M6c intracerebral tumors. *F*, young female C3(1)/Tag transgenic mice (~7 weeks old) bearing intracerebral M6c tumors were injected at the same coordinates with G47Δ (2 × 10⁶ pfu/4 μL; *n* = 9) or Mock (*n* = 12) and the animals were sacrificed when moribund. G47Δ significantly extended survival [*P* = 0.003; log-rank (Mantel-Cox) test]. Mean survival was increased from 16 days for Mock to 24 days for G47Δ. *G*, M6c cells (4 × 10⁵ cells) were injected stereotactically into aged female C3(1)/Tag transgenic mice (9 months old) and treated 10 days later with G47Δ (*n* = 10) or Mock (*n* = 9). More cells were injected because older mice tend to have lower take rates than young mice. G47Δ significantly extended survival [*P* < 0.005; log-rank (Mantel-Cox) test]. Mean survival was increased from 17 days for Mock to 21 days for G47Δ. *H*, M6c cells (2 × 10⁵) were injected stereotactically into female C3(1)/Tag transgenic mice (~2 months old), 10 days later NV1023 (*n* = 8), NV1042 (*n* = 11; 2 × 10⁶ pfu/4 μL), or Mock (PBS/10% glycerol; *n* = 11) were injected at the same coordinates and the animals were sacrificed when moribund. NV1023 significantly extended survival compared with Mock [*P* = 0.004; log-rank (Mantel-Cox) test], whereas NV1042 was barely significant [*P* = 0.05; log-rank (Mantel-Cox) test]. Mean survival was increased from 14 days for Mock to 20 days for NV1023 and 18 days for NV1042.

s.c. tumor model, extending mean survival to 20 days from 14 days for Mock. NV1042 only extended survival to 18 days. In this experiment, the survival of G47Δ treated mice was similar to the NV1042 treated mice (data not shown). All mice that were sacrificed or died had brain tumors.

Spontaneously Arising Mammary Tumors. In our hands, female heterozygous mice develop palpable tumors from about 3 to 5.5 months of age (Fig. 3*A*), although the penetrance is <80%. A mouse with multiple mammary tumors at 6 months of age is illustrated in Fig. 3*B*. G47Δ replication in the tumors could be detected after intratumoral injection from 2 days (Fig. 3*C*) to 7 days post-treatment, with only a few positive cells seen at day 14. Because mammary tumors arise over a period of time and each mouse develops different numbers of tumors, we used three treatment strategies. In the first, mice were randomly divided into two groups (G47Δ and Mock) when the first mammary tumor was palpable. This tumor was injected once a week and tumor size determined twice a week (Fig. 4*A*). There was a high degree of variability in the tumor growth rates in the Mock-treated tumors; however, almost half the tumors exhibited rapid

growth to a very large size (Fig. 4*A*, *right*), whereas, none of the G47Δ-treated tumors exhibited such growth and many had somewhat stable disease (Fig. 4*A*, *middle*). The mean tumor volume of the G47Δ-treated tumors was less than the Mock-treated tumors (Fig. 4*A*, *left*). Animals were sacrificed when the tumor burden became too large, with the growth of untreated tumors often leading to the sacrifice of the G47Δ-treated mice. Therefore, there were no apparent treatment effects on survival. There was also no significant difference in the number of mammary tumors arising between the G47Δ (mean = 5.7) and Mock (mean = 5.1) groups.

In the second experiment, all tumors were treated when they became palpable, with the mice randomized to treatment groups when the first tumor emerged. These groups also included mice with multiple tumors at the time of first treatment or mice bearing ectopic tumors, those that could not be definitively identified as mammary tumors (i.e., tumors on the neck, flank, and shoulder that could have arisen from sweat glands). In this case, we have treated each tumor as an independent entity and found that G47Δ significantly increased the time to tumor progression (Fig. 4*B*).
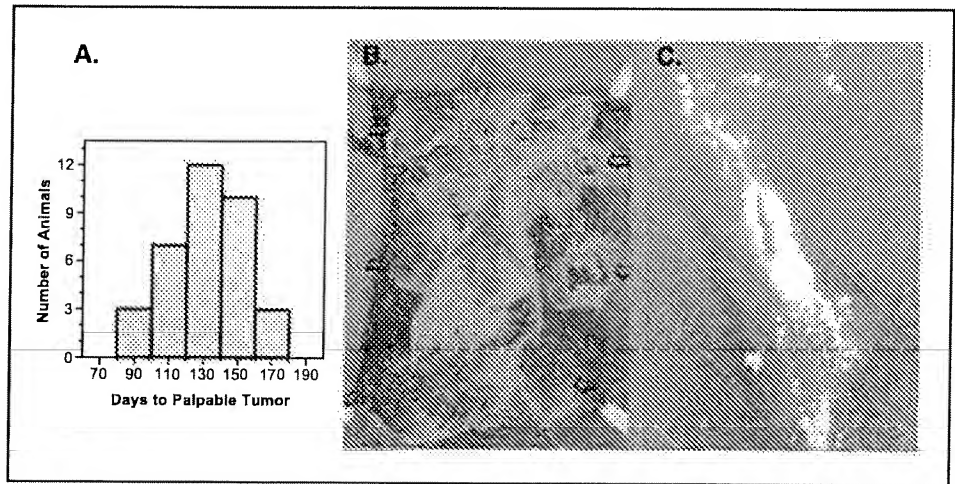
Figure 3. Spontaneously arising mammary tumors in C3(1)/T-Ag heterozygous transgenic mice. *A.* time course of tumor development, with the age when the first palpable tumor detected is plotted. *B.* necropsy of mouse (6 months of age) with multiple large mammary tumors (*arrow*). *C.* viral spread in spontaneous mammary tumor after intratumoral inoculation. G47Δ (2 × 10⁷ pfu) was injected into a large mammary tumor(1.4 cm³) that was removed 2 days later, sectioned, and stained with X-gal histochemistry.

In the final treatment paradigm, we treated the first mammary tumor to arise and then surgically removed the other nine breast tissues. In this case, we were able to follow the growth of the injected tumors, for the most part without the confounding effects of subsequent arising tumors. G47Δ did not appreciably inhibit tumor growth, although we were able to follow mean growth longer than for Mock (Fig. 5, *left*). NV1042 did significantly inhibit tumor growth compared with both Mock and G47Δ and delayed tumor progression by over 2.5 times compared with Mock (Fig. 5, *right*). Whereas neither G47Δ nor NV1042 significantly extended overall survival in this experiment, median survival increased from 5.5 weeks for Mock to 8.5 and 9 weeks for G47Δ and NV1042 respectively. Many of these mice were sacrificed due to ectopic tumor burden (usually on the neck or vagina); 62% of Mock, 29% of G47Δ, and 43% of NV1042. All of the Mock-treated tumors progressed to >10 times their initial treatment volume (to ~1,000 mm³), whereas, only four of seven tumors (57%) in the G47Δ and NV1042 groups progressed to that size. The difference in time to progression to 10 times the initial volume was not quite significant (P = 0.06; log-rank test). The effects of G47Δ intratumoral injection on spontaneous mammary tumor growth was not large, but consistent between the different treatment paradigms. The enhanced efficacy of NV1042, consistent with the s.c. tumor study, is supportive of the view that local IL-12 expression improves oncolytic HSV efficacy.

Discussion

Virotherapy, the use of viruses to treat cancer, has been resurrected as a cancer therapy strategy within the last dozen years (8). To target tumor cells and spare normal cells, most of the oncolytic HSV vectors have deletions/mutations in one or more of the genes affecting neurovirulence (*UL56* and *γ34.5*), replication in nondividing cells (*UL39*), or inhibition of protein kinase R pathway activation (γ34.5; ref. 9). Over 20 different oncolytic HSV vectors have been evaluated in a large variety of different tumor types and models (9). Among these 1716, G207, and NV1020 have been translated to the clinic for the treatment of melanoma, malignant glioma, and metastatic colorectal cancer (9). In these studies, we compared the efficacy of G207, its derivative G47Δ, NV1023, and its IL-12 expressing derivative NV1042 in the C3(1)/T-Ag transgenic breast cancer model (Table 1).

Various oncolytic HSV vectors have been tested in both human xenograft and mouse syngeneic models of breast cancer, usually with metastatic disease (38, 40–42). For example, intratumoral injection of murine 4T1 primary tumors with HSV-1 1716 or Synco-2D resulted in a significant reduction in lung metastases (41, 42). The efficacy of G207 and NV1020, the parental viruses of G47Δ and NV1023, have been previously compared in a number of different tumor models, including human pancreatic, gastric, and prostate cancer, and mouse bladder and colorectal cancer (28, 43–46). In most cases, both viruses were similarly effective, and the differences seemed to be tumor cell and not tumor type specific. For example, with human head and neck squamous cell carcinoma cell lines, both G207 and NV1020 caused complete regression of nearly all s.c. SSC15 tumors, whereas G207 was ineffective at inhibiting s.c. SCC1483 growth (47), whereas NV1020 was very efficacious (26). Here we found that both G207 and NV1023, derived from NV1020, were ineffective at inhibiting s.c. M6c tumor growth, and G207 was not examined further in the C3(1)/T-Ag transgenic model.

The tumor environment, including surrounding normal cells and extracellular matrix, plays an important role in tumor growth (48) and therapeutic efficacy (49). Differences between the brain parenchyma and the s.c. space may have contributed to the efficacy of NV1023 in treating intracerebral tumors and

<table>
<tr><td colspan="4">**Table 1.** Summary of oncolytic HSV vector efficacy on M6c tumors from C3(1)/T-Ag mice</td></tr>
<tr><td>Virus</td><td colspan="2">S.c.</td><td>Intracerebral</td></tr>
<tr><td></td><td>Tumor growth</td><td>Survival</td><td>Survival</td></tr>
<tr><td>G207</td><td>No</td><td>No</td><td>ND*</td></tr>
<tr><td>G47Δ</td><td>Yes†</td><td>Yes</td><td>Yes</td></tr>
<tr><td>NV1023</td><td>No</td><td>No</td><td>Yes</td></tr>
<tr><td>NV1042 (IL-12)</td><td>Yes</td><td>Yes</td><td>Yes</td></tr>
</table>

*Not done.
†Statistically significant difference from Mock treatment (P < 0.05).

Figure 4. Treatment of spontaneously arising mammary tumors in C3(1)/T-Ag transgenic mice. *A*, first spontaneous mammary tumor (palpable) was treated with an intratumoral injection of G47Δ (1×10^7 pfu in 20 μL; $n = 8$) or Mock (PBS/10% glycerol; $n = 9$) and weekly thereafter until the mice were sacrificed due to overall tumor burden. Tumor volume = length × width × height. *Left*, whereas the mean tumor volumes of G47Δ treated tumors are smaller than Mock, the difference is not significant ($P \le 0.07$ at weeks 0.5, 1, 1.5, 3.5, and 4; unpaired *t* test). However, the slopes of the best-fit lines are significantly different ($P < 0.001$). Because the tumors were measured twice a week, the midweek measurements for different animals could vary by a day; however, they were grouped for purposes of determining the means. *Bars*, standard error of the mean. *Right*, growths of individual treated tumors are plotted. *B*, every spontaneously arising tumor (when it became palpable) was injected with G47Δ ($n = 18$ in six mice) or Mock ($n = 26$ in six mice) weekly and tumor size measured. The time to progression to 2.2 times the original volume at initial treatment (80-420 mm³) is plotted. G47Δ significantly inhibited tumor progression compared with Mock [$P < 0.01$; log-rank (Mantel-Cox) and Wilcoxon rank tests].
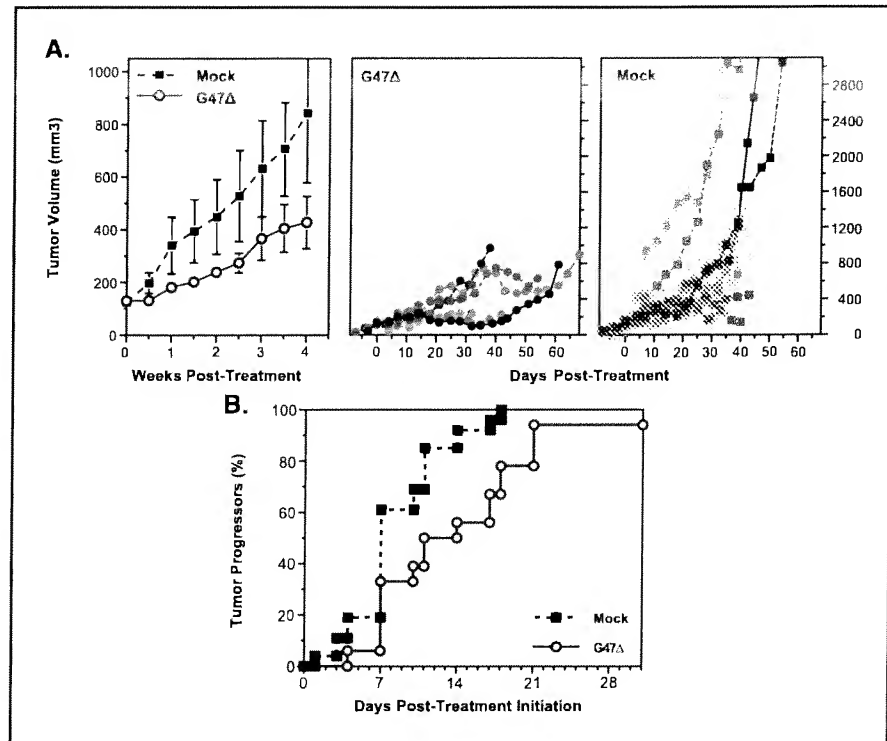
not s.c. tumors. For many biological therapeutic strategies, the complex stromal-tumor interactions that develop during tumor progression and the generation of immune tolerance against tumor antigens are important features that are not fully operative in implanted tumor models. Genetically engineered mice that spontaneously develop tumors are some of the most representative models we currently have for human cancer, both in furthering our understanding of disease progression and for the preclinical evaluation of new therapies (50). Unfortunately, these tumor models are much more difficult to work with and successfully treat than typical implant models.

In the C3(1)/T-Ag transgenic mouse, the C3(1) regulatory region drives expression of SV40 large and small T-Ag in mammary epithelial ductal cells and the terminal ductal lobular unit (33, 35).

Whereas SV40 T-Ag is not expressed in human breast cancer, it inactivates the p53 and Rb pathways that are commonly mutated in breast cancer (51). Heterozygous female C3(1)/T-Ag develop mammary adenocarcinomas, which histologically resembles human breast cancer usually classified as infiltrating ductal carcinoma (34). Although the C3(1) regulatory region contains hormone response elements (52), T-Ag expression is not estrogen responsive. The mouse tumors have up-regulated expression of TGF-α, Her2/neu, and c-myc and loss of ER-α expression (35). In patients, low ER-α expression is associated with less differentiated, more aggressive, and more difficult to treat tumors. In our studies, we found an incomplete penetrance of tumor formation, with <80% of mice developing tumors, as opposed to the 100% reported in the literature (34), which may reflect epigenetic factors. Genetic polymorphisms

Figure 5. Oncolytic HSV treatment of single spontaneously arising C3(1)/T-Ag mammary carcinomas. The first spontaneously arising mammary tumor was inoculated with G47Δ or NV1042 (2×10^7 pfu in 20 μL) or Mock (PBS/10% glycerol in 20 μL) weekly. Following the first treatment, the remaining mammary glands were surgically removed. *Left*, tumor growth was followed until the overall tumor burden became too large and the mean tumor volume determined ($n = 8$ for Mock and $n = 7$ for NV1042 and G47Δ). NV1042 is more efficacious at inhibiting tumor growth than G47Δ, which was similar to Mock in this experiment, although the difference compared with Mock is only significant at early time points. *, $P < 0.02$ (unpaired *t* test). *Bars*, standard deviation from the mean. *Right*, time to progression to 2.2 times the initial treatment volume. NV1042 significantly delays tumor progression compared with Mock [$P < 0.02$, log-rank (Mantel-Cox)].
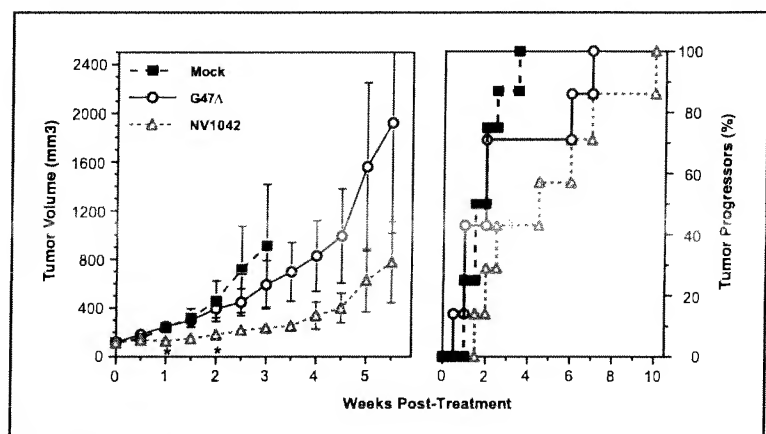
may also play a role, as a recent report described the loss of tumor development after breeding on the C57BL background (53).

The availability of tumor cell lines from the C3(1)/T-Ag mice further enhances their utility, providing the means to perform studies *in vitro* and to rapidly screen agents in syngeneic implant models. Tumor cell lines M6 (derived from a spontaneous mammary carcinoma) and M6c (derived from a lung metastasis of an implanted s.c. M6 tumor) both retain expression of the oncogenic transgene (T-Ag; ref. 36), like the spontaneously arising tumors *in vivo* (33). Therefore, they only form tumors in immune-deficient or heterozygous transgenic mice, with tolerance to T-Ag. When M6c cells were implanted into nontransgenic parental FVB/N mice by mistake, no tumors were formed. We found that the M6c cells were more susceptible than the M6 cells to oncolytic HSV replication *in vitro* and that the M6 cells had highly variable rates of s.c. tumor growth *in vivo*. In addition, the M6c cells formed multifocal tumors when implanted into the brain, providing a model for metastatic breast cancer to the brain. In all three C3(1)/T-Ag cell lines, G47Δ was more cytotoxic than G207 at low MOI, whereas at high MOI G207 was able to kill both the M6c and M6 cells. This enhanced cytotoxicity *in vitro* of G47Δ at low MOI is seen in most tumor cell lines tested (19).[1]

The C3(1)/T-Ag transgenic mouse has proven to be a useful model of breast cancer for the evaluation of experimental therapeutics and chemopreventive agents. A range of chemo-preventive agents (retinoids, difluoromethylornithine, dehydroepi-androsterone, and nonsteroidal anti-inflammatory drugs) have been shown to inhibit tumor development, most likely at the progression to invasive carcinoma stage (54). The goal of our studies was to treat established carcinomas that were palpable by direct intratumoral injection. To our knowledge, this is the first description of virotherapy in a transgenic spontaneously arising tumor model. The studies were confounded by the highly variable rates of measurable tumor growth and development of multiple tumors. We tried three different experimental para-digms to accommodate the variable number and time of initiation of tumors. In the first, only the first palpable mammary tumor to arise was treated and all tumors followed for growth. Alternatively, all tumors were treated when they became palpable. We did not detect any effect of G47Δ treatment on the growth of nontreated tumors, or the time of appearance of subsequent tumors, or on the total number of tumors. We have not tried to optimize therapeutic efficacy by altering the treatment paradigm, but based on previous studies in other models, this should be possible.

IL-12 is a proinflammatory cytokine at the intersection of innate and adaptive immunity that has broad antitumor activities, including inducing IFN-γ production, which up-regulates MHC class I and chemokine (IP-10 and MIG) expression, nitric oxide production, and inhibition of angiogen-esis; differentiating CD4+ Th1 cells and inducing opsonizing antibodies; and activating CTL and NKT cells (55). We and others have shown that IL-12 expression is very effective at augmenting the antitumor efficacy of oncolytic HSV vectors. IL-12 has been given as a recombinant protein in combination with G207 (56), expressed from a defective HSV vector in combination with G207 (31), or as a transgene encoded

by the oncolytic vector (30, 32), as described here. The enhanced efficacy of NV1042 over NV1023 in squamous cell carcinoma was dependent upon CD4+/CD8+ lymphocytes (30). We found that the effect of local IL-12 expression varied depending upon tumor location. NV1042 (IL-12+) was more efficacious than NV1023 in the periphery (s.c. and autochthonous), but less in the brain, possibly due to its immune privileged status. In contrast, M002, another oncolytic HSV vector expressing IL-12, significantly extended the survival of mice bearing intracerebral Neuro2a tumors in A/J mice when compared with its parent virus (32).

Administration of rIL-12 with weekly doses of rIL-2 (pulse IL-2) to C3(1)/T-Ag transgenic mice with palpable or multifocal tumors resulted in inhibition of tumor growth, tumor regression in mice with smaller tumor burden, and decreased tumor number (57). However, tumors arose after cessation of treatment, indicating that an effective memory immune response was not generated, and treatment of juvenile mice delayed the appearance of tumors, but did not block their development (57). IL-12 in this system was suggested to be inhibiting angiogenesis, rather than enhancing an immune response. In contrast, rIL-12 did not inhibit angiogenesis or autochthonous tumor growth in a MMTV-induced mammary carcinoma model, whereas it did with implanted Mm5Mt cells (established from a mouse mammary tumor virus–induced mam-mary carcinoma; ref. 58), further illustrating the difference between *in situ* arising and implanted tumors. We have not examined the effect of oncolytic HSV or IL-12 on angiogenesis, but NV1042 was recently reported to have antiangiogenic activity in a squamous cell carcinoma model (59).

Direct antiangiogenic factors have also shown significant efficacy in inhibiting mammary tumor growth in C3(1)/T-Ag transgenic mice. Both recombinant mouse endostatin and the human P125A mutant, and VEGF-DT385 toxin inhibited tumor growth and number, and extended survival when given before tumor appear-ance, although all mice succumbed to disease (60–62). In a gene therapy strategy, i.v. delivery of adenovirus vectors expressing mouse endostatin inhibited cumulative tumor volume, but to a lesser extent than recombinant endostatin (63). Other transgenic mouse breast cancer models have also been used to test various therapeutic agents, again, usually before tumor appearance. The MMTV neu transgenic mouse has been used to test a variety of antiestrogen and antiangiogenic factors (including plasmids encoding angiostatin, endostatin, TIMP-2, sFLT-1, and IFN-α) and combinations of them (64). The combination of tamoxifen with rIL-12 was very effective at preventing carcinoma development in the Her2/neu transgenic mouse (65), likely due again to the antiangio-genic properties of IL-12.

Oncolytic viruses in general and HSV vectors in particular have been applied to the treatment of a large variety of cancers: however, there has been less experimentation with breast cancer. Primary breast tumors can be successfully treated by surgery if they are localized. Unfortunately, many tumors are not caught at an early stage and metastatic and/or hormone insensitive disease ensues, for which treatment is much less effective. C3(1)/T-Ag transgenic mice provide an excellent model for the development and testing of novel therapeutics. While the spontaneous adenocarcinomas are extremely difficult to treat pharmacologically and are non-immunogenic in syngeneic hosts, similar to the clinical situation, we have shown that the third generation oncolytic HSV vector G47Δ has efficacy both in established brain metastases and spontaneous primary tumors, and the IL-12 expressing vector NV1042 was the most effective vector in the periphery.

---

[1] Unpublished data.

Acknowledgments

References

1. Weir HK, Thun MJ, Hankey BF, et al. Annual report to the nation on the status of cancer, 1975-2000, featuring the uses of surveillance data for cancer prevention and control. J Natl Cancer Inst 2003;95:1276-99.

2. Jemal A, Clegg LX, Ward E, et al. Annual report to the nation on the status of cancer, 1975-2001, with a special feature regarding survival. Cancer 2004;101:3-27.

3. Boogerd W. Central nervous system metastasis in breast cancer. Radiother Oncol 1996;40:5-22.

4. Crivellari D, Pagani O, Veronesi A, et al. High incidence of central nervous system involvement in patients with metastatic or locally advanced breast cancer treated with epirubicin and docetaxel. Ann Oncol 2001;12:353-6.

5. Hortobagyi GN. Treatment of breast cancer. N Engl J Med 1998;339:974-84.

6. Baselga J, Norton L. Focus on breast cancer. Cancer Cell 2002;1:319-22.

7. Mahmoud-Ahmed AS, Suh JH, Lee SY, Crownover RL, Barnett GH. Results of whole brain radiotherapy in patients with brain metastases from breast cancer: a retrospective study. Int J Radiat Oncol Biol Phys 2002;54:810-7.

8. Kirn D, Martuza RL, Zwiebel J. Replication-selective virotherapy for cancer: biological principles, risk management and future directions. Nat Med 2001;7:781-7.

9. Varghese S, Rabkin SD. Oncolytic herpes simplex virus vectors for cancer virotherapy. Cancer Gene Ther 2002;9:967-78.

10. Chou J, Kern ER, Whitley RJ, Roizman B. Mapping of herpes simplex virus-1 neurovirulence to γ 34.5, a gene nonessential for growth in culture. Science 1990;250:1262-6.

11. He B, Gross M, Roizman B. The γ(1)34.5 protein of herpes simplex virus 1 complexes with protein phosphatase 1α to dephosphorylate the α subunit of the eukaryotic translation initiation factor 2 and preclude the shutoff of protein synthesis by double-stranded RNA-activated protein kinase. Proc Natl Acad Sci U S A 1997;94:843-8.

12. Goldstein DJ, Weller SK. Herpes simplex virus type 1-induced ribonucleotide reductase activity is dispensible for virus growth and DNA synthesis: isolation and characterization of an ICP6 lacZ insertion mutant. J Virol 1988;62:196-205.

13. Mineta T, Rabkin SD, Yazaki T, Hunter WD, Martuza RL. Attenuated multi-mutated herpes simplex virus-1 for the treatment of malignant gliomas. Nature Medicine 1995;1:938-43.

14. Todo T, Ebright MI, Fong Y, Rabkin SD. Oncolytic herpes simplex virus (G207) therapy: from basic to clinical. In: Maruta H, editor. Tumor-suppressing viruses, genes, and drugs. San Diego: Academic Press, 2002. p. 45-75.

15. Toda M, Rabkin SD, Kojima H, Martuza RL. Herpes simplex virus as an *in situ* cancer vaccine for the induction of specific anti-tumor immunity. Hum Gene Ther 1999;10:385-93.

16. Todo T, Rabkin SD, Sundaresan P, et al. Systemic antitumor immunity in experimental brain tumor therapy using a multimutated, replication-competent herpes simplex virus. Hum Gene Ther 1999;10:2741-55.

17. Nakano K, Todo T, Chijiiwa K, Tanaka M. Therapeutic efficacy of G207, a conditionally replicating herpes simplex virus type 1 mutant, for gallbladder carcinoma in immunocompetent hamsters. Mol Ther 2001;3:431-7.

18. Endo T, Toda M, Watanabe M, et al. *In situ* cancer vaccination with a replication-conditional HSV for the treatment of liver metastasis of colon cancer. Cancer Gene Ther 2002;9:142-8.

19. Todo T, Martuza RL, Rabkin SD, Johnson PA. Oncolytic herpes simplex virus vector with enhanced MHC class I presentation and tumor cell killing. Proc Natl Acad Sci U S A 2001;98:6396-401.

20. Mohr I, Gluzman Y. A herpes virus genetic element which affects translation in the absence of the viral GADD34 function. EMBO J 1996;15:4759-66.

21. York IA, Roop C, Andrews DW, Riddell SR, Graham FL, Johnson DC. A cytosolic herpes simplex virus protein inhibits antigen presentation to CD8+ T lymphocytes. Cell 1994;77:525-35.

22. Huard B, Früh K. A role for MHC class I downregulation in NK cell lysis of herpes virus-infected cells. Eur J Immunol 2000;30:509-15.

23. Jugovic P, Hill AM, Tomazin R, Ploegh H, Johnson DC. Inhibition of major histocompatibility complex class I antigen presentation in pig and primate cells by herpes simplex virus type 1 and 2 ICP47. J Virol 1998;72:5076-84.

24. Meignier B, Longnecker R, Roizman B. *In vivo* behavior of genetically engineered herpes simplex viruses R7017 and R7020: construction and evaluation in rodents. J Infect Dis 1988;158:602-14.

25. Whitley RJ, Roizman B. Herpes simplex viruses: is a vaccine tenable? J Clin Invest 2002;110:145-51.

26. Wong RJ, Kim SH, Joe JK, Shah JP, Johnson PA, Fong Y. Effective treatment of head and neck squamous cell carcinoma by an oncolytic herpes simplex virus. J Am Coll Surg 2001;193:12-21.

27. Advani SJ, Chung SM, Yan SY, et al. Replication-competent, nonneuroinvasive genetically engineered herpes virus is highly effective in the treatment of therapy-resistant experimental human tumors. Cancer Res 1999;59:2055-8.

28. Delman KA, Bennett JJ, Zager JS, et al. Effects of preexisting immunity on the response to herpes simplex-based oncolytic viral therapy. Hum Gene Ther 2000;11:2465-72.

29. Fong Y, Kemeny N, Jarnagin W, et al. Phase I study of a replication-competent herpes simplex oncolytic virus for treatment of hepatic colorectal metastases. Am Soc Clin Oncol Ann Mtg 2002:27.

30. Wong RJ, Patel SG, Kim S, et al. Cytokine gene transfer enhances herpes oncolytic therapy in murine squamous cell carcinoma. Hum Gene Ther 2001;12:253-65.

31. Toda M, Martuza RL, Kojima H, Rabkin SD. *In situ* cancer vaccination: an IL-12 defective vector/replication-competent herpes simplex virus combination induces local and systemic antitumor activity. J Immunol 1998;160:4457-64.

32. Parker JN, Gillespie GY, Love CE, Randall S, Whitley RJ, Markert JM. Engineered herpes simplex virus expressing IL-12 in the treatment of experimental murine brain tumors. Proc Natl Acad Sci U S A 2000;97:2208-13.

33. Maroulakou IG, Anver M, Garrett L, Green JE. Prostate and mammary adenocarcinoma in transgenic mice carrying a rat C3(1) simian virus 40 large tumor antigen fusion gene. Proc Natl Acad Sci U S A 1994;91:11236-40.

34. Green JE, Shibata MA, Yoshidome K, et al. The C3(1)/SV40 T-antigen transgenic mouse model of mammary cancer: ductal epithelial cell targeting with multistage progression to carcinoma. Oncogene 2000;19:1020-7.

35. Yoshidome K, Shibata MA, Couldrey C, Korach KS, Green JE. Estrogen promotes mammary tumor development in C3(1)/SV40 large T-antigen transgenic mice: paradoxical loss of estrogen receptor α

36. Holzer RG, MacDougall C, Cortright G, Atwood K, Green JE, Jorcyk CL. Development and characterization of a progressive series of mammary adenocarcinoma cell lines derived from the C3(1)/SV40 large T-antigen transgenic mouse model. Breast Cancer Res Treat 2003;77:65-76.

37. Jorcyk CL, Liu ML, Shibata MA, et al. Development and characterization of a mouse prostate adenocarcinoma cell line: ductal formation determined by extracellular matrix. Prostate 1998;34:10-22.

38. Toda M, Rabkin SD, Martuza RL. Treatment of human breast cancer in a brain metastatic model by G207, a replication-competent multimutated herpes simplex virus 1. Hum Gene Ther 1998;9:2177-85.

39. James K, Eisenhauer E, Christian M, et al. Measuring response in solid tumors: unidimensional versus bidimensional measurement. J Natl Cancer Inst 1999;91:523-8.

40. Wu A, Mazumder A, Martuza RL, et al. Biological purging of breast cancer cells using an attenuated replication-competent herpes simplex virus in human hematopoietic stem cell transplantation. Cancer Res 2001;61:3009-15.

41. Thomas DL, Fraser NW. HSV-1 therapy of primary tumors reduces the number of metastases in an immune-competent model of metastatic breast cancer. Mol Ther 2003;8:543-51.

42. Nakamori M, Fu X, Rousseau R, Chen SY, Zhang X. Destruction of nonimmunogenic mammary tumor cells by a fusogenic oncolytic herpes simplex virus induces potent antitumor immunity. Mol Ther 2004;9:658-65.

43. McAuliffe PF, Jarnagin WR, Johnson P, Delman KA, Federoff H, Fong Y. Effective treatment of pancreatic tumors with two multimutated herpes simplex oncolytic viruses. J Gastrointest Surg 2000;4:580-8.

44. Bennett JJ, Delman KA, Burt BM, et al. Comparison of safety, delivery, and efficacy of two oncolytic herpes viruses (G207 and NV1020) for peritoneal cancer. Cancer Gene Ther 2002;9:935-45.

45. Cozzi PJ, Burke PB, Bhargav A, et al. Oncolytic viral gene therapy for prostate cancer using two attenuated, replication-competent, genetically engineered herpes simplex viruses. Prostate 2002;53:95-100.

46. Cozzi PJ, Malhotra S, McAuliffe P, et al. Intravesical oncolytic viral therapy using attenuated, replication-competent herpes simplex viruses G207 and Nv1020 is effective in the treatment of bladder cancer in an orthotopic syngeneic model. FASEB J 2001;15:1306-8.

47. Carew JF, Kooby DA, Halterman MW, Federoff HJ, Fong Y. Selective infection and cytolysis of human head and neck squamous cell carcinoma with sparing of normal mucosa by a cytotoxic herpes simplex virus type 1 (G207). Hum Gene Ther 1999;10:1599-606.

48. Bissell MJ, Radisky D. Putting tumours in context. Nat Rev Cancer 2001;1:46-54.

49. Bibby MC. Orthotopic models of cancer for preclinical drug evaluation: advantages and disadvantages. Eur J Cancer 2004;40:852-7.

50. Hansen K, Khanna C. Spontaneous and genetically engineered animal models: use in preclinical cancer drug development. Eur J Cancer 2004;40:858-80.

51. Geradts J, Ingram CD. Abnormal expression of cell cycle regulatory proteins in ductal and lobular carcinomas of the breast. Mod Pathol 2000;13:945-53.

52. Page MJ, Parker MG. Effect of androgen on the transcription of rat prostatic binding protein genes. Mol Cell Endocrinol 1982;27:343-55.

53. Verschoyle RD, Edwards R, Nolan B, Greaves P. Articular chondromatosis and chondroid metaplasia in transgenic TAg mice. Toxicol Pathol 2004;32:22-5.

54. Kavanaugh C, Green JE. The use of genetically altered mice for breast cancer prevention studies. J Nutr 2003;133:2404–9S.

55. Trinchieri G. Interleukin-12 and the regulation of innate resistance and adaptive immunity. Nat Rev Immunol 2003;3:133–46.

56. Iizuka Y, Suzuki A, Kawakami Y, Toda M. Augmentation of antitumor immune responses by multiple intratumoral inoculations of replication-conditional HSV and interleukin-12. J Immunother 2004;27:92–8.

57. Wigginton JM, Park JW, Gruys ME, et al. Complete regression of established spontaneous mammary carcinoma and the therapeutic prevention of genetically programmed neoplastic transition by IL-12/pulse IL-2: induction of local T cell infiltration, Fas/Fas ligand gene expression, and mammary epithelial apoptosis. J Immunol 2001;166:1156–68.

58. Lee JC, Kim DC, Gee MS, et al. Interleukin-12 inhibits angiogenesis and growth of transplanted but not *in situ* mouse mammary tumor virus-induced mammary carcinomas. Cancer Res 2002;62:747–55.

59. Wong RJ, Chan MK, Yu Z, et al. Angiogenesis inhibition by an oncolytic herpes virus expressing interleukin 12. Clin Cancer Res 2004;10:4509–16.

60. Yokoyama Y, Green JE, Sukhatme VP, Ramakrishnan S. Effect of endostatin on spontaneous tumorigenesis of mammary adenocarcinoma in a transgenic mouse model. Cancer Res 2000;60:4362–5.

61. Calvo A, Yokoyama Y, Smith LE, et al. Inhibition of the mammary carcinoma angiogenic switch in C3(1)/SV40 transgenic mice by a mutated form of human endostatin. Int J Cancer 2002;101:224–34.

62. Wild R, Yokoyama Y, Dings RP, Ramakrishnan S. VEGF-DT385 toxin conjugate inhibits mammary ade-

nocarcinoma development in a transgenic mouse model of spontaneous tumorigenesis. Breast Cancer Res Treat 2004;85:161–71.

63. Calvo A, Feldman AL, Libutti SK, Green JE. Adenovirus-mediated endostatin delivery results in inhibition of mammary gland tumor growth in C3(1)/SV40 T-antigen transgenic mice. Cancer Res 2002;62:3934–8.

64. Sacco MG, Soldati S, Indraccolo S, et al. Combined antiestrogen, antiangiogenic and anti-invasion therapy inhibits primary and metastatic tumor growth in the MMTVneu model of breast cancer. Gene Ther 2003;10:1903–9.

65. Nanni P, Nicoletti G, De Giovanni C, et al. Prevention of HER-2/neu transgenic mammary carcinoma by tamoxifen plus interleukin 12. Int J Cancer 2003;105:384–9.